

'Thermal forces': colloids in temperature gradients

This article has been downloaded from IOPscience. Please scroll down to see the full text article.

2004 J. Phys.: Condens. Matter 16 S4195

(<http://iopscience.iop.org/0953-8984/16/38/032>)

View [the table of contents for this issue](#), or go to the [journal homepage](#) for more

Download details:

IP Address: 129.252.86.83

The article was downloaded on 27/05/2010 at 17:47

Please note that [terms and conditions apply](#).

‘Thermal forces’: colloids in temperature gradients

Roberto Piazza

Dipartimento di Ingegneria Nucleare, Politecnico di Milano, via Ponzio 34/3, 30133 Milano, Italy

E-mail: roberto.piazza@polimi.it

Received 13 April 2004

Published 10 September 2004

Online at stacks.iop.org/JPhysCM/16/S4195

doi:10.1088/0953-8984/16/38/032

Abstract

In the presence of a thermal gradient, macromolecular solutes or dispersed particles drift to the cold or to the hot side: this effect is known as thermophoresis, and is the counterpart of particle suspensions of the Soret effect (or thermal diffusion) in simple fluid mixtures. Here I review recent experimental results on colloid thermophoresis and present new data suggesting a universal nature for the temperature dependence of thermophoresis in aqueous systems. There are strong analogies between thermophoresis in liquids and other thermally induced flow processes like gas thermal creep and membrane thermo-osmosis; starting from these, I present some guidelines for a general model of thermophoresis in disperse systems, accounting both for single-particle and collective effects.

1. Introduction

The analysis of the behaviour of colloidal dispersions in external fields or in non-equilibrium conditions may shed additional light on many features of the structural and dynamic behaviour of disperse systems that are still just partly understood. For instance, while accurate experimental investigation methods like scattering techniques probe *colligative* properties, field-induced colloid transport properties often depend on single-particle properties, and in particular on particle–solvent interactions; since the specific nature of the potential of the mean force eventually stems from particle solvation properties, detailed analysis of the latter is crucial for colloidal science.

Thermophoresis, consisting in the drift of dispersed particles driven by a thermal gradient, is the counterpart of macromolecular solutions or colloidal suspensions of thermal diffusion (or the Ludwig–Soret effect [1]) in simple fluid mixtures [2]. Particle thermophoresis takes place not only in liquids but also in gases, where it has been extensively investigated due to its important practical consequences [3]. Conversely, although preliminary investigations were performed back in 1977 [4], particle thermophoresis in liquids has been only marginally explored, outstanding exceptions being detailed studies of polymer solutions [5] and

ferrofluids [6]. The potential practical impact of thermophoretic effects has been recently marked out by brilliant experiments on DNA solutions [7], showing that thermophoresis may concur with thermal convection in leading to patterns where the local solute concentration is amplified up to a thousand fold.

Yet, physical understanding of thermophoresis is so far very poor. Even the direction of particle motion looks ‘erratic’: in most cases colloids migrate towards the cold, displaying what we shall call ‘thermophobic’ behaviour, but examples of ‘thermophilic’ motion (along the temperature gradient) have often been reported [4, 8, 9]. In dilute suspensions (particle weight fraction $w \ll 1$), the mass flow J can be written as $J = -D\nabla c - cD_T\nabla T$, where c is the particle concentration in mass per unit volume, D is the usual Brownian diffusion coefficient, and D_T is called the coefficient of thermal diffusion. In the absence of convection, and assuming that ∇T is directed along z , Soret-coupling of heat and mass transfer leads therefore to a steady-state concentration gradient given by

$$\frac{dc}{dz} = -cS_T\frac{dT}{dz}, \quad (1)$$

where $S_T = D_T/D$ is called the Soret coefficient. With the present definition, S_T is therefore positive for thermophobic particle motion. It is also useful to introduce the thermal diffusion ratio $k_T = (Tc/\rho_S)S_T$ (where ρ_S is the solution mass density), which is a pure number.

Here we shall exclusively deal with thermophoresis colloidal suspensions and macromolecular solutions, although some basic concepts underlying thermally driven motion in gases will be presented for comparison; the specific purpose of the paper will indeed be trying to single out possible microscopic mechanisms of thermophoresis, drawing connections to other non-equilibrium transport effects induced by thermal gradients and relating them to basic structural aspects of inhomogeneous fluids. The paper is organized as follows:

- I shall first describe two optical methods we use to investigate thermophoresis, and review some of the recent work recently performed by our group on macromolecular solutions and colloidal dispersions.
- After a short discussion of thermally driven particle transport in gases, specifically aimed to find parallels with thermophoresis in liquids, I will then try using some basic considerations made by Derjaguin [10, 11] and Ruckenstein [12] to build a general model for thermophoresis, which stresses the key role of particle/solvent interfacial properties in setting the nature of single-particle thermophoretic motion.
- Finally, the single-particle model will be generalized to take into account collective properties that, as we shall see, deeply influence thermophoresis.

2. Experimental aspects

Let me first give a short description of the two experimental techniques we use, both originally applied by Giglio and Vendramini [4, 13] to investigate Soret effects, which we will refer to as the *beam-deflection* and the *thermal-lens* methods.

The beam-deflection (BD) method exploits the deflection of a laser beam due to the concentration, and therefore refractive index gradient induced by the imposed temperature field. Suppose for instance that the combined effects of solvent thermal expansivity and solute thermal diffusion lead to a refractive index gradient pointing downwards: the lower portion of a planar wavefront is then delayed compared to its upper part, and the beam suffers an overall downward deflection. Our experimental apparatus [14] consists first of all of a thermal-diffusion cell, made of two horizontal closely spaced (0.6 mm) plates separated by an optical-glass frame, with an optical path length of 40 mm and a sample volume of about

300 μl . Tuning of plate temperatures is achieved using two independently controlled Peltier modules, placed in close thermal contact with the plates. Typically, a temperature difference $\Delta T \simeq 0.5\text{--}1^\circ\text{C}$ between the initially isothermal plates is applied in a timescale of a few tens of seconds, and kept fixed within 5 mK for up to several hours. A laser beam is mildly focused through the plate gap, and the position of the transmitted beam is monitored by a position-sensitive detector (PSD) with a resolution of a few μm , placed far from the cell. The beam suffers first a very rapid downward deflection $(\Delta z)_{\text{th}}$ due to the temperature dependence of the refractive index of the solution, followed by a much slower change $\Delta z_{\text{S}}(t)$ due to the progressive build-up of the Soret-induced concentration gradient, reaching exponentially an asymptotic limit $(\Delta z)_{\text{S}}$ with a time constant τ set by the particle Brownian diffusion time over the plate separation distance. The thermal diffusion ratio is simply determined as

$$k_{\text{T}} = -T \frac{\partial n / \partial T}{\partial n / \partial w} \frac{(\Delta z)_{\text{S}}}{(\Delta z)_{\text{th}}}. \quad (2)$$

It is interesting to note that direct comparison of the angular displacements of the solution versus the pure solvent yield an internal calibration with no reference to the apparatus geometry.

BD is therefore a simple, reliable, and accurate method. However, it has a major drawback: since the plate spacing cannot be made much smaller than about 1 mm, diffusion times τ are quite long (hours), even for particles with size in the few nm range. Measurements on suspensions of monodisperse spherical latex particles, which are typically at least one order of magnitude larger, are therefore precluded. All-optical methods, where laser beams are used in concert for heating up the sample and detecting concentration gradients driven by the Soret effect, conversely allow setting thermal gradients on very small spatial scales. Thermal lensing (TL) [15] is a self-effect on beam propagation taking place when a focused laser beam heats up a partially absorbing medium, generating a locally inhomogeneous refractive index profile acting as a negative lens, which in turn increases the divergence of the transmitted beam. In fluid mixtures or solutions, the laser-induced temperature profile also drives Soret motion, which leads to the progressive buildup of a concentration gradient within the heated region, acting as an additional lens-like element. This ‘Soret lens’ can be divergent or convergent depending on the preferential direction of motion of the component having the largest index of refraction, and as a result spreading of the transmitted beam may further increase, or conversely lessen. However, visible lasers cannot be used to induce TL in aqueous suspensions, since water is highly transparent through the whole visible range. Measurements of the Soret effect by TL methods have been therefore limited to strongly absorbing mixtures, like in the original experiments by Giglio and Vendramini [13], or have relied on adding to the suspension an absorbing dye, which may, however, introduce some complications. The main novelty of our apparatus is that we use a near-infrared laser, tuned to match a small vibrational overtone peak of water. Since the focused beam has a spot of a few tens of μm , measurement timescales are considerably shorter than for the BD method. There is, however, a specific feature of the TL method requiring careful consideration. At variance with BD, a radially symmetric laser beam unavoidably sets *horizontal* temperature gradients: this means that convection effects are inescapable. The basic strategy to limit their effects is reducing the focused spot so that on its spatial scale diffusion is much faster than convection, so that a safe criterium is keeping $wU/D \ll 1$, where w is the beam-spot size and U is the typical convection velocity that can be evaluated by balancing viscous and buoyancy forces. A detailed description of our experimental apparatus and an extensive analysis of convective effects can be found in [16]. Here we only point out that, using our experimental configuration, the Soret coefficient of polystyrene latex particles with radius $R = 100\text{ nm}$ ($D \simeq 2 \times 10^{-8}\text{ cm}^2\text{ s}^{-1}$) can be easily measured with a very good degree of accuracy and reproducibility.

Using the aforementioned methods, in the last few years we have tried to concentrate on colloidal systems that can be regarded as ‘model’ systems to investigate the basic features of particle thermophoresis. We shall primarily discuss the results obtained for two specific systems, which have been selected in consideration of their well-known structural properties:

- Ionic surfactant solutions, where the surfactant micelles act as small, globular charged particles, and the interparticle interactions, primarily of electrostatic nature, can be easily tuned by the addition of salt.
- Protein solutions, where the potential of the mean force displays a simple, very short-ranged attractive term that can be easily tuned by changing temperature.

The equilibrium structural and dynamic properties of SDS solutions have been studied at length in the past. In particular, SDS micelles can be modelled as spherical aggregates of radius $R \approx 2.5$ nm, interacting via a standard DLVO potential [17]. By measuring the Soret coefficient of charged SDS micelles, Piazza and Guarino have shown that thermophoresis in SDS solutions has a very distinctive behaviour. In the limit of very low concentration, S_T sensibly drops by adding salt. In other words, the single-particle Soret effect strongly increases with the electrostatic Debye–Hückel screening length λ_{DH} . However, intermicellar interactions play a strongly conflicting role, to such an extent that even at moderately low SDS concentration the situation gets totally reversed, and S_T *increases* with increasing salt concentration c_S . Quantitatively, the single-particle Soret coefficient S_{T0} is found to scale as the square of λ_{DH} . Collective effects show the same ionic-strength dependence as the solution osmotic compressibility: they increase, or conversely reduce the Soret coefficient compared to S_{T0} depending on the fact that intermicellar interactions are, respectively, attractive or repulsive.

Proteins in ‘salting-out’ conditions, that is in the presence of a sufficient amount of added salt, display strongly temperature-dependent solution properties [19]. In the last few years, lysozyme has become a kind of ‘benchmark’ for testing the basic features of the phase behaviour of globular proteins. By measuring the Soret coefficient of hen egg-white lysozyme solutions, Iacopini and Piazza [8] have shown a very peculiar aspect of thermophoresis in protein solutions: particle motion can indeed be tuned from thermophobic to thermophilic by decreasing temperature. Moreover, the absolute value of S_T increases exponentially with decreasing temperature, with a growth parameter that weakly depends on the ionic strength. Finally, a strong correlation of S_T with lysozyme equilibrium solubility was observed. Recently [20], we have further expanded the analysis to include effects of particle charge and of the addition of different salts, and analysed the transient effect to derive the temperature dependence of the thermal diffusion coefficient D_T , which was found to grow *linearly* with temperature, showing as S_T sign-reversal at a temperature that weakly depends on pH or ionic strength.

Observing that, at variance with simple charged colloids, proteins generally display a large exposed hydrophobic surface area, we originally tried ascribing these puzzling temperature effects to the strong temperature dependence of hydrophobic interactions. Here, however, we are performing measurements suggesting that a very similar behaviour is shared by a wide class of aqueous dispersed systems, ranging from polypeptides to synthetic polyelectrolytes, micelles and even rigid latex particles [21]. In figure 1, for instance, we show the temperature dependence of the Soret coefficient for SDS micelles, obtained for two different surfactant concentrations at the same value of the solution ionic strength. At variance with the results obtained in [8] for lysozyme solutions, SDS behaviour is found to be ‘thermophobic’ in the whole investigated temperature range (which had to be limited to T higher than the SDS ‘Kraft point’ $T_K \simeq 5$ °C, the temperature where the surfactant crystallizes out from solution).

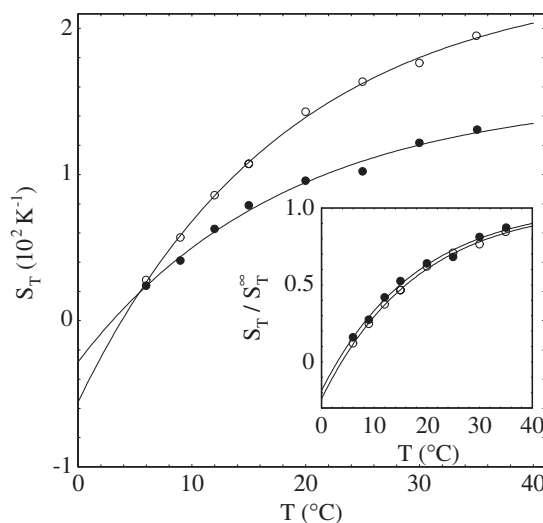


Figure 1. Temperature dependence of the Soret coefficient S_T for SDS solutions at surfactant concentration $c = 10 \text{ g ml}^{-1}$ (open dots) and $c = 19 \text{ g ml}^{-1}$ (full dots), in the presence of 10 mM NaCl, fitted according to equation (3). Fit parameter values (S_T^∞ (K^{-1}), T^* ($^\circ\text{C}$), T_0 ($^\circ\text{C}$)) are given by [2.36, 3.8, 18.1] ($c = 10 \text{ g ml}^{-1}$) and [1.55, 3.0, 18.0] ($c = 19 \text{ g ml}^{-1}$). Curves are rescaled in the inset by S_T^∞ .

However, the experimental points are fitted quite well using the same empirical function suggested in [8]

$$S_T(T) = S_T^\infty \left[1 - \exp\left(\frac{T^* - T}{T_0}\right) \right], \quad (3)$$

with an extrapolated sign-reversal temperature T^* close to 3–4 $^\circ\text{C}$. Moreover, increasing the total surfactant concentration (and therefore the strength of repulsive intermicellar interactions) reduces the overall amplitude of the effect, but has little effect on T^* and T_0 : this is evident from the inset, where both curves are rescaled to their asymptotic value S_T^∞ . The reversal temperature and the rate of change for S_T seem therefore to be single-particle properties, which are not influenced by interparticle interactions.

3. Intermezzo: thermophoresis in gases

Although this topic lies outside the specific purposes of the present paper, it is particularly instructive skimming through the origin of forces on solid surfaces induced by thermal gradients in gases. This is actually a long story, dating back to 1873, when Sir William Crookes developed a special tool, consisting of a vertical low-friction rotor with four vanes blackened on one side and silvered on the other, originally meant to detect light pressure (figure 2). As is well known from basic courses on experimental physics, unless very high vacuum is made in the glass container, the Crookes ‘radiometer’ does not live up to its purpose: it turns the ‘wrong’ way around, with the black surfaces pushed away by the light¹.

A comprehensive account of the heated debate triggered by the radiometer can be found in the historical review by Brush [22], while a clear and still illuminating analysis of motion in rarefied gases was made back in 1938 by Kennard [23]. Yet, unfortunately, the explanation of

¹ It is interesting to notice that Maxwell himself originally accepted Crookes’ explanation in terms of radiation pressure, but he very soon repented, as we shall see.

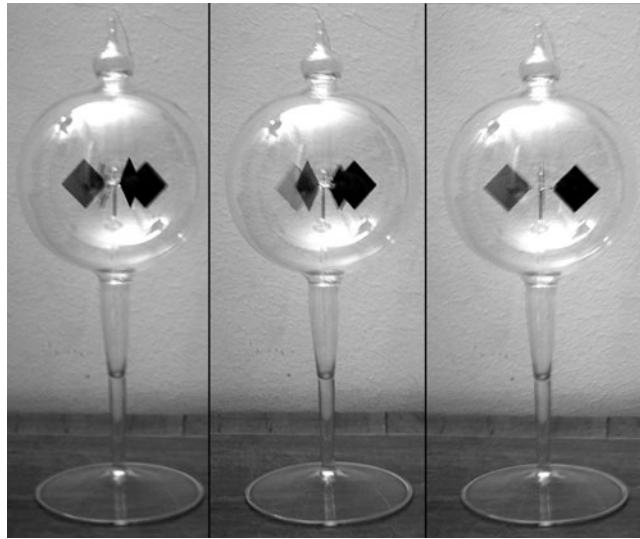


Figure 2. A Crookes radiometer, spinning in the author's living room.

this effect still presented in many books, including the *Encyclopædia Britannica*, is definitely wrong. The argument goes as follows: the black side of the van heats the surrounding gas molecule, which therefore acquire kinetic energy and 'kick' the black side more strongly. Of course, this is nonsense. To have a stationary gas, we need equalization of *pressure*: therefore, near the black side we have a hotter, but less dense gas, giving the same normal component of momentum transfer to the vane. Even in the presence of convection things do not change: convection patterns around a vertical heated surface do not display transverse pressure gradients, and there is no pressure drop between the thermal boundary layers and the bulk, stationary gas. Why therefore, provided that the gas pressure in the radiometer is sufficiently low, do the vanes turn? Amendment by Maxwell came with his last paper published in 1879 [24], where he took advantage of the seminal explanation by Osborne Reynolds of gas 'thermal transpiration' through porous membranes to give the correct explanation: the radiometer turns because of *tangential* stresses present at the *edges* of the vanes².

Let us try recasting Maxwell's argument in modern terms. In the presence of a thermal gradient, corrections to the equilibrium distribution $f_0(v)$ of the molecule speed (which *must* be included in order to account for dissipative processes like heat transport) can be evaluated from the Boltzmann equation. Taking x as the direction of the thermal gradient, at first order we can write [23]

$$f(v) = f_0[1 + Cv_x(5/2 - mv^2/2k_B T)], \quad (4)$$

where m is the molecular mass and C is a normalization constant. It is easy to show that, in bulk, the non-equilibrium distribution (4) does not lead to longitudinal transfer of momentum. However, let us assume that the gas is bounded by a solid planar surface S , with a temperature gradient along the plane, and consider those molecules that lie within a mean free path λ from S . Molecular impacts with a solid surface are not specular reflection, and the velocity distribution after the impact will be partly thermalized: although exact expressions for what is called the

² Actually, the publishing of Maxwell's paper was a sort of *casus belli*. Maxwell had been the referee of Reynolds' paper: unfortunately, publication of the latter was delayed, and followed Maxwell's work. Reynolds, obviously, did not like it. Today, luckily, such things never happen...

‘accommodation coefficient’ are not easily evaluated, and depends on the specific model for the surface, there is in any case a partial transfer of momentum to the wall. Yet, molecules coming from the hot side carry more momentum than those coming from the cold, and therefore a net *longitudinal* momentum transfer takes place. This mechanism, besides accounting for Crookes radiometer motion (although, clearly, quantitative evaluation is hard) and explaining gas ‘thermal creep’ in pores, can be invoked for giving a first semi-quantitative explanation of particle thermophoresis in gases, an effect originally discovered by Tyndall [25]. In the near-continuum limit (the situation is very different in the extremely dilute, or ‘Knudsen’, regime), a first solution was given by Epstein [26], who calculated a particle thermophoretic velocity for a particle with thermal conductivity κ_P , embedded in a gas having thermal conductivity κ_g and number density ρ .

$$v_{\text{th}} = \frac{3\eta}{2\rho T} \left(\frac{\kappa_g}{2\kappa_g + \kappa_P} \right) \nabla T_0, \quad (5)$$

where m is the molecular mass and the term in bracket accounts for the particle-induced modification of the externally imposed gradient ∇T_0 . By relating the gas viscosity to the mean free path via $\eta = (m/2k_B T)^{1/2} p \lambda = (m/2k_B T)^{1/2} \rho k_B T \lambda$, we have

$$v_{\text{th}} = \sqrt{\frac{9k_B}{8mT}} \lambda \left(\frac{\kappa_g}{2\kappa_g + \kappa_P} \right) \nabla T_0, \quad (6)$$

showing that the thermophoretic velocity is proportional to λ (so that, as we stated previously, the effect is more relevant at low pressure). The Epstein approach was further refined by other researchers to include higher order terms, which extended the solutions from the near-continuum to the full Knudsen regime [3]. Although we cannot dwell more on the latter rather complex subject, it is useful for what follows to stress some key aspects of the Reynolds–Maxwell mechanism:

- The gas exerts on the surface (or vice versa) a *tangential* stress. In a continuum description, this corresponds to having a pressure tensor near the surface which is anisotropic in the direction of the thermal gradient.
- The inhomogeneous gas region where the velocity distribution differs from the equilibrium value is confined within a surface layer with a thickness of the order of λ : the mean free path acts therefore as a *characteristic length scale* controlling the amplitude of the effect.
- From a macroscopic point of view, thermophoresis can be seen as an effective *slip* of the particle, that is a violation of the hydrodynamic stick boundary condition confined within a mean free path from the surface.
- Particle *bulk* properties enter the problem only through the thermal conductivity κ_P that, in relation to κ_g , yields the local distortion of the temperature field.

As we shall see, these points bear a strong resemblance to the analogous features of particle thermophoresis in liquids.

4. ‘Phoretic’ transport phenomena in liquids

We have, first of all, to stress a basic distinction between two different kinds of colloid transport phenomena in external fields. In the first case, the field couples directly to the particle acting as a *volume* force, gravitational sedimentation being the simplest example. However, let us consider electrophoresis, namely the transport of charged colloids induced by an external electric field. The particle is surrounded by the small ion double-layer, extending up to a distance from the particle surface which is of the order of the Debye–Hückel screening length λ_{DH} : therefore, when observed over hydrodynamic length scales, which are generally quite

larger than λ_{DH} , no net electric force is applied to the particle/double-layer system, which appears overall neutral. In addition, if the field is sufficiently weak, distortion (polarization) of the double-layer is negligible, and the counterion/coion cloud retains its zero-field distribution. Why, then, do the particles move? The driving force stems from a relative motion of the fluid with respect to the particle that is localized within the double-layer. Since the double-layer, which we shall call the ‘internal region’ of the fluid, is very thin, on the hydrodynamic scale this relative motion may be described as a ‘slip’ of the fluid on the particle surface. In other words, *the existence of a diffuse interface (the internal region) between the fluid and the solid surface can be represented as an effective violation of the no-slip condition.*

This peculiar coupling is therefore basically an *interfacial* stress effect, and is responsible for what we shall call, in general, *phoretic* motion [27]. Calculation of the flow-field proceeds therefore in principle by determining the flow in the internal region, evaluating the slip at the particle surface, and plugging it as an effective boundary condition in the Navier–Stokes equations. It is evident therefore that phoretic effects directly probe the particle–solvent interactions: the presence of the particle surface, acting as an effective external field, modifies the local structure of the solvent structure in the interfacial region. In a continuum picture, as we shall see, this effect can be described as the onset of interfacial tension gradients driving the particle motion; phoretic effects for a solid particle surrounded by a *diffuse* fluid interface are therefore similar to ‘Marangoni’ effects taking place at a sharp *macroscopic* fluid–fluid interface (in particular thermophoresis could be seen, as we shall discuss, as a kind of microscopic thermocapillary effect).

Actually, phoretic effects are not necessarily associated with the presence of a ‘real’ external field: conversely, colloidal motion driven by interfacial stresses can also be brought about by gradients of thermodynamic quantities. For instance, charged colloid motion can be induced by concentration gradients of electrolytes as in dielectrophoresis, by pH gradients for particle with basic or acidic surface groups, or in general by the inhomogeneous distribution of low-molecular weight solutes: all these phenomena (which can collectively be named ‘diffusiophoretic’ effects) can be described using concepts that are very similar to those we have just introduced. Thermophoresis, as we shall see, is another (and probably simpler) example. Conceptually, however, the situation is very different. While for electrophoresis interfacial stresses come out as the overall effect of well defined electric forces on each single component (particle and small ions), here we are considering non-equilibrium systems where no ‘external field’ coupling with the particle or the low molecular weight components is present. The key question about phoretic motion driven by thermodynamic gradients is therefore: *can we ‘map’ our non-equilibrium suspension onto an ‘effective’ equilibrium system subjected to an appropriate ‘fictitious’ external field?* For the specific case of thermophoresis, this means ‘translating’ the effect of the thermal inhomogeneity of the solvent into an effective mechanical disturbance inducing particle flow, eventually balanced by the usual osmotic flow to yield a steady-state concentration gradient.

5. Towards a general model of thermophoresis

Let me first state explicitly the framework and limitations of the model I shall present in what follows. The analysis will be strictly limited to particle/solvent interaction with a range *much smaller* than the particle size. The ‘internal region’ we shall try to characterize is therefore very thin, so that on its scale the particle surface appears as *flat*. This greatly simplifies the approach, allowing the extraction of information on particle thermophoresis from other flow effects taking place for a thermally inhomogeneous liquid bounded by solid surfaces. So far, ‘curvature’ effects due to finite particle size proved indeed much harder to be included: unfortunately, as

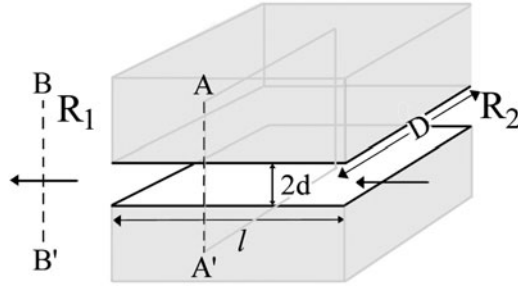


Figure 3. Schematic geometry for the calculation of the thermo-osmotic effects in the model presented in [11].

we are presently finding for latex particles at very low ionic strength ($\lambda_{\text{DH}} \gg R$), these effects seem to be much stronger than in the case of electrophoresis.

5.1. The Derjaguin approach to thermo-osmosis and thermophoresis

At variance with what has been done for electrophoresis and diffusiophoresis, very limited theoretical work has so far been done on thermophoresis in liquids. The only existing general model of particle transport in thermal gradients is due to Derjaguin and Sidorenkov [10, 11], who tackled the problem of thermophoresis (or, more precisely, thermo-osmosis, i.e. thermally driven flow of liquids near solid surfaces) by considering the reciprocal mechano-caloric effect, namely the buildup of thermal gradients due to fluid flow in capillary pores, using then Onsager reciprocal relations. Let us briefly recall the main steps of their derivation of the thermophoretic velocity. Consider the fluid flow through a straight capillary of length l with a rectangular cross-section, connecting two reservoirs R_1 and R_2 . We shall assume that pressure and temperature differences ΔP , ΔT are externally imposed between the reservoirs and, to simplify calculation, we shall take the capillary height $2d$ much smaller than its width D (see figure 3).

The fluid-volume and heat flows, J_V (in $\text{m}^3 \text{s}^{-1}$) and J_Q (in J s^{-1}), may be written in terms of generalized forces as:

$$\begin{aligned} J_V &= \beta_{11} \Delta P + \beta_{12} \frac{\Delta T}{T} \\ J_Q &= \beta_{21} \Delta P + \beta_{22} \frac{\Delta T}{T} \end{aligned} \quad (7)$$

where the coefficients $\beta_{12,21}$ yield the amplitude of the cross-flows. Suppose now that, due to interactions with the pore walls, the fluid structure in the pore differs from the bulk: in particular, we write the local specific enthalpy as $h_0 + \Delta h(z)$, where h_0 is the bulk value. When $\Delta T = 0$, the excess heat flow through any section AA' in the capillary (yielding at steady state a temperature difference between the reservoirs) is given by:

$$W_{AA'} = h_0 J_V + D \int_{-d}^d \Delta h(z) v(z) dz \quad (8)$$

where $v(z)$ is the fluid velocity in the pore. Taking for the latter a Poiseuille form $v(z) = (z^2 - d^2) \Delta P / \eta l$ we get

$$\beta_{21} = \frac{D}{\eta l} \int_{-d}^d \Delta h(z) (z^2 - d^2) dz = \beta_{12}, \quad (9)$$

where the last identity is a consequence of Onsager reciprocity relations. Expression (9) can be simplified by taking into account that the thickness of the internal region δ is much smaller

than h and linearizing the Poiseuille velocity field in the distance z' from the wall, obtaining

$$\beta_{12} = -\frac{2S}{\eta l} h^1 \quad (10)$$

where $S = 2Dd$ is the capillary cross-section, and

$$h^1 = \int_0^\delta \Delta h(z) z \, dz \quad (11)$$

is the first moment of the distribution of the excess enthalpy in the internal region. The slip velocity is then simply obtained dividing J_V by the capillary cross-section

$$v_s = -2 \frac{h^1}{\eta T} \nabla T, \quad (12)$$

where $\nabla T = \Delta T/l$ is the temperature gradient. Obviously, provided that the fluid inhomogeneous region is thin compared to the particle size, the steady-state thermophoretic velocity acquired by a particle driven a thermal gradient in a stationary fluid is simply given by $v_{th} = -v_s$.

The thermophoretic velocity can also be written as

$$v_{th} = 2 \frac{h_s \ell}{\eta T} \nabla T, \quad (13)$$

where $h_s \equiv \int_0^\delta \Delta h'(z) \, dz$ is the excess enthalpy per unit surface, and $\ell \equiv h_s^{-1} h^1$ is a characteristic length scale. The latter expression allows for a simple qualitative understanding of the thermophoretic behaviour. When the colloid–particle interactions are attractive (the particle surface is ‘lyophilic’), so that the excess enthalpy in the internal region is everywhere negative, the particle diffuses to the cold; conversely, for repulsive fluid–surface interactions (‘lyophobic’ colloids), a thermophilic behaviour is expected. The situation is slightly more complicated if the excess enthalpy in the internal region has not everywhere the same sign (for instance, when the particle/wall interactions are repulsive at short range and attractive at longer distance, or vice versa). Here ℓ , which in the former case is positive definite, may be negative as well, and can even switch sign if the range of one of the two terms in the surface interaction potential changes, for instance, with temperature.

The close relation between thermo-osmosis and thermophoresis is given further support by considering the experimental evidence collected many years ago by Haase and De Greiff [29]. The experiment consists in measuring the steady-state pressure difference ΔP between two reservoirs kept at different temperatures and separated by a porous membrane, and calculating from it the ‘heat of transport’, which in our notation is given by $Q^* = \beta_{12}/\beta_{11} = -T(\Delta P/\Delta T)_{J_V=0}$, and should therefore be proportional to the slip velocity v_s (or to $-v_{th}$).³ In particular, Haase and De Greiff measured the dependence of Q^* on the average system temperature for water transport through cellophane membranes, which is shown (with reversed sign) in figure 4. Resemblance with the experimental results in [8] for the temperature dependence of the Soret coefficient (and therefore the thermophoretic velocity) for lysozyme solutions is striking: not only does $-Q^*$ change in sign from negative to positive by increasing T , but its functional dependence on T can be fitted over the whole investigated range using an empirical expression which is identical to that proposed for thermophoresis by Iacopini and Piazza:

$$Q^*(T) = Q_\infty^* \left[\exp\left(\frac{T^* - T}{T_0}\right) - 1 \right], \quad (14)$$

³ Notice, however, that this method works better for small β_{11} , that is for thin pores, where the approximation used to derive (10) is no longer valid.

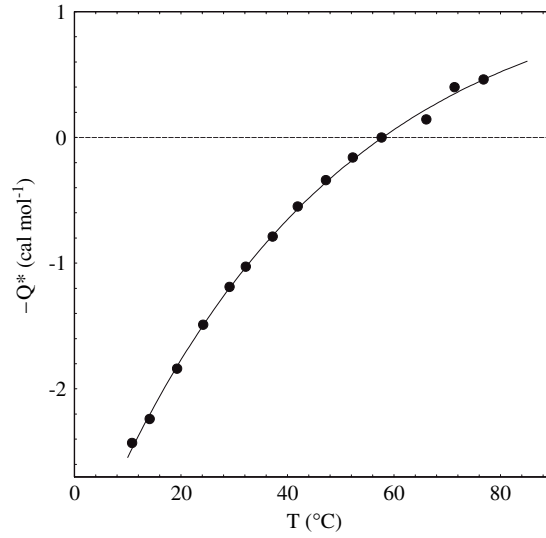


Figure 4. Heat of transport of water through cellophane membranes as a function of the mean system temperature (after [29]). The full curve is a fit with the empirical expression used by Iacopini and Piazza for the temperature dependence of the Soret coefficients in protein solutions.

where Q_{∞}^* represents a high- T limit, $T \simeq 57$ °C is the temperature where the heat of transport switches sign, and T_0 embodies the strength of temperature effects. It is also interesting to point out that the characteristic energy scale $k_B T_0$ has the same order of magnitude found for thermophoresis, namely about 15% of the thermal energy.

A note of caution concerns, however, the correct interpretation of the excess enthalpy term. Equation (10) comes from the evaluation of *integrated* flows (along the full length of the capillary) using an approach which is typical for *discontinuous* systems. In a later analysis of thermo-osmotic flow in semipermeable membranes, Dariel and Kedern [28] pointed out that the total heat of transport can be written as $Q^* = Q_m + \Delta H^s$, where Q_m is the effective heat transported within the membrane and ΔH^s is an additional contribution due to the enthalpy of fluid transfer from the bulk to the pore (or, equivalently, to the excess enthalpy originating from immersing the membrane in the fluid). To reach this conclusion, Dariel and Kedern start from the *local* flux equations at a given cross-section of the pore, which can be written as

$$\begin{aligned} J_m &= l_{11} \left(\frac{d\mu}{dx} \right)_T + \frac{l_{12}}{T} \frac{dT}{dx} \\ J_q &= l_{21} \left(\frac{d\mu}{dx} \right)_T + \frac{l_{22}}{T} \frac{dT}{dx} \end{aligned} \quad (15)$$

where J_m is the mass flow (in moles per unit time) across a given section of the capillary, and $(d\mu/dx)_T$ is the chemical potential gradient at constant T within the pore. Using *this* local form of the coupled-flow equations, Onsager reciprocal relations yield $l_{12} \equiv l_{21}$. By integrating equations (15) along the capillary, and carefully considering boundary conditions (in particular matching of the chemical potential difference between the reservoirs, obtained either by direct balance or by integrating (15)), Derjaguin equations (15) are retained provided that (equation (27) by Dariel and Kedern, in our notation)

$$\beta_{12} = \beta_{21} - \Delta H^s V_m l_{11} / l \quad (16)$$

where V_m is the fluid molar volume. Taking into account that, in isothermal conditions, the volume flow is given by $J_V = (l_{11} V_m / l) \Delta p$, the second term on the rhs of equation (16) is easily seen to correspond to a flux of enthalpy taken up at R_1 and released at R_2 , without contributing to the homogeneous energy transfer within the pore (this occurrence of excess surface terms in passing from continuous to discontinuous flow equations is discussed at length in [28]). The author must confess that his own acquaintance with membrane-exchange thermodynamics is too limited to judge whether this conclusion is correct, but the argument is sound. From a practical point of view, this observation simply means that the excess enthalpy due to the creation of the interface should not be included in equation (11) so that we must consequently write

$$h^1 = \int_0^\delta \Delta h'(z) z \, dz \quad (17)$$

where $\Delta h'(z) = \Delta h(z) - \Delta h_0(z)$ and $\Delta h_0(z)$ is the distribution of the isothermal excess enthalpy in the internal region.

5.2. Interfacial tension and phoretic motion

A step forward can be made by drawing a connection between phoretic effects and the interfacial thermodynamic properties expressed in terms of a macroscopic interfacial tension γ . Let us first observe that, for the specific case of thermophoresis or thermo-osmosis, the enthalpy per unit surface appearing in (13) should be regarded as the excess part with respect to the condition of zero thermal gradient. In the presence of a bounding surface of area S , a simple thermodynamic relation links the enthalpy H of the fluid to the interfacial tension γ

$$H = H_0 + \left(\gamma - T \frac{d\gamma}{dT} \right) S. \quad (18)$$

Besides the bulk term H_0 , the first term in brackets corresponds to the excess enthalpy due only the presence of the wall, even in the absence of a temperature gradient. If the observation made in [28] is correct, this term should consequently be discarded. Therefore, the only excess contribution per unit surface due to ΔT is

$$h_s = -T \frac{d\gamma}{dT}, \quad (19)$$

yielding a thermophoretic velocity

$$v_{th} = -\frac{2\ell}{\eta} \gamma'(T) \nabla T = -\frac{2\ell}{\eta} \frac{d\gamma}{dx}, \quad (20)$$

where $\gamma'(T) = d\gamma/dT$ and x is the coordinate along the interface. Connection between gradients of the interfacial tension and phoretic motion is, however, very general [27]. It is indeed well known that fluid pressure near an interface is no longer isotropic. For a flat interface, the pressure tensor has only two independent terms: the normal component p_N , coinciding everywhere with the bulk pressure, and a tangential component $p_T(z)$, where z is the distance from the substrate, smaller than p_N and often negative (i.e. a tangential *tension*). The interfacial tension is simply given (this is almost a definition of γ) by [30]

$$\gamma = \int_0^\infty dz [p_N - p_T(z)]. \quad (21)$$

Now, in the presence of a gradient of a thermodynamic quantity, like for instance temperature, p_T will vary along the interface. In stationary conditions, we can write the balance of pressure and viscous shear stresses as

$$\frac{\partial \sigma_{zx}}{\partial z} + \frac{\partial P^*}{\partial x} = 0, \quad (22)$$

where $P^*(x, z) = p_N - p_T(x, z)$. Using (21), the total stress discontinuity τ through the internal region, driving phoretic motion, is therefore given by:

$$\tau = \sigma_{zx}(+\infty) - \sigma_{zx}(0) = -d\gamma/dx. \quad (23)$$

Once the dependence of P^* on the inhomogeneous thermodynamic parameter is known, the slip velocity can therefore be evaluated by integrating twice (22) and evaluating the velocity field at the outer boundary of the internal region (it should be noted that, due to the thinness of the internal region, the velocity field reaches its asymptotic value rather fast [27]).

5.3. Ruckenstein model for thermophoresis of charged colloids

The considerations made in the former section give firmer bases to a clever intuition by Eli Ruckenstein about the general mechanism of phoretic motion in suspensions of charged colloids [12], later exploited and extended by Piazza and Guarino to explain the general features of thermophoresis in charged micellar solutions [18]. In his seminal paper, Ruckenstein notices that, in the limit of a thin double-layer, the electrophoretic velocity v_E along z for a colloidal particle with surface charge density σ and surface potential ψ_s can be written as

$$v_E = \frac{-\lambda_D H}{\eta} \frac{d\gamma}{dz}, \quad (24)$$

where η and ϵ are the solvent viscosity and dielectric constant, and ℓ is a characteristic length, which in the Debye–Hückel limit ($\psi_s/k_B T \ll 1$) coincides with $\lambda_D H$. The interfacial tension γ between particle and solvent can be calculated from the work needed to build up the double-layer [31]

$$\gamma_{el} = - \int_0^{\psi_s} \sigma d\psi. \quad (25)$$

Within the same limit of low surface potential, $\sigma = (\epsilon/4\pi\lambda_{DH})\psi_s$, so that

$$\gamma_{el} = -\epsilon\psi_s^2/8\pi\lambda_{DH}. \quad (26)$$

By simultaneously solving the Navier–Stokes and Gibbs adsorption equations, Ruckenstein then shows that an expression similar to (24) holds for diffusiophoresis and thermophoresis as well, provided that we choose $\ell = \lambda_{DH}/2$ and that $d\gamma/dz$ is appropriately related to the presence of chemical or temperature gradients.

Piazza and Guarino suggested that the same approach may also be used for higher surface potentials, provided that the effective (or renormalized) charge Z_{eff} [32] is substituted for the bare charge Z . In physical terms, this amounts to assuming that the ‘condensed’ counterions are so strongly bound to the particle surface that they do not participate in the slip motion of the internal region, or equivalently, that the ζ -potential (the electrostatic potential at the ‘plane of shear’) is of the order of $k_B T$. If this ansatz holds true, the Soret coefficient can then be easily found by calculating the thermophoretic velocity v_{th} and setting to zero the net particle flux $J = \rho v_{\text{th}} - D_0 \nabla \rho$, where ρ is the colloid number density, obtaining

$$S_T = S_T^{\text{NE}} + \frac{3\pi l_B Z^2}{4TR^3} \lambda_{DH}^2, \quad (27)$$

where R is the particle radius, l_B is the Bjerrum length, and a possible additional contribution S_T^{NE} to S_T due to particle–solvent interactions of non-electrostatic nature has been added to the electrostatic term. Equation (27) accounts therefore for the observed scaling of the Soret coefficient with the square of λ_{DH} . In addition, if we evaluate the amplitude of the quadratic term by using a ‘dressed’ micellar radius $R = 3.5$ nm and the effective charge value $Z_{\text{eff}} \approx 17$ obtained in [33], equation (27) closely fits the data obtained for SDS micelles.

Equation (27), however, should be valid only when λ_{DH} is not too large compared to the particle size. In the case of SDS micelles, the screening length cannot be made too large due to the screening effect of free, non-micellized surfactant, present at a residual concentration approximately equal to the critical micellar concentration (cmc): since the cmc can be as large as 8 g l^{-1} in the absence of added salt, this effect is far from being negligible. Preliminary data obtained with the TL method on strongly interacting polystyrene latex spheres show that at very low ionic strength the situation could be much more complicated, showing even a reversal in sign of the Soret coefficient. This feature is actually predicted by a more elaborate analysis of charged colloid thermophoresis [34]. However, the latter model requires extensive and rather cumbersome numerical calculation, and does not yield any simple physical intuition of the origin of S_T sign reversal.

5.4. ‘Thermal force’ and bulk effects

Both the general model we developed from the Derjaguin approach in section 5.2 and the specific suggestion made by Derjaguin yield a thermophoretic velocity scaling as $v_{\text{th}} = -(\ell/\eta)\gamma'(T)\nabla T$, where the characteristic length scale ℓ is related, according to the previous discussion, to the solvent structure in the internal region, and eventually to the specific particle–solvent interactions. This expression for v_{th} simply corresponds, however, to the stationary velocity that a particle of radius R would attain in the presence of an ‘effective external field’

$$F_{\text{th}} = -A\ell\gamma'(T)\nabla T \quad (28)$$

where A is a dimensionless constant. F_{th} plays therefore the role of the ‘thermal force’ we were looking for.

Expression (28) confirms that the Soret effect is essentially related to interfacial properties: we may wonder, however, whether *bulk* particle properties have any effect on thermophoresis. As a matter of fact, bulk properties modify indeed the local thermal gradient: due to the formal identity of the constitutive equations, the temperature profile around a particle having thermal conductivity κ_P , embedded in a solvent with thermal conductivity κ_S , can be directly evaluated by analogy with the problem of the electric polarization of a non-conductive particle immersed in a dielectric [35], obtaining

$$\nabla T(r) = \left[1 - \frac{\kappa_P - \kappa_S}{\kappa_P + 2\kappa_S} \left(\frac{r}{R} \right)^3 \right] \nabla T_0, \quad (29)$$

where ∇T_0 is the unperturbed, externally imposed thermal gradient and r is the distance from the particle centre, so that the effective thermal gradient at the particle surface is simply rescaled to $\nabla T(R) = 3\kappa_S/(\kappa_P + 2\kappa_S)\nabla T_0$. The amplitude A of the thermal force in (28) should therefore be proportional to $3\kappa_S/(\kappa_P + 2\kappa_S)$ (exactly as in Epstein’s solution for thermophoresis in gases), being particularly large for highly thermally conductive solvents.

6. Collective effects

So far we have neglected any effect colloidal interparticle interactions and limited our analysis to single-particle effects. However, the chance of ‘translating’ the thermal gradient into an effective external ‘driving force’ given by (28) allows for a simple generalization of the model to take into account collective effects. Without F_{th} , steady-state would be reached when the osmotic pressure Π as a function of the local temperature and concentration, is constant along the cell (this is a simple consequence of the McMillan–Mayer theory for dilute solutions, since Π takes the place of the hydrostatic pressure, which must be uniform in mechanical equilibrium). In the presence of the thermal force, the ‘hydrostatic’ balance is given by

$$\nabla \Pi = -A\ell\rho\gamma'(T)\nabla T \quad (30)$$

where ρ is the local particle number density. Expanding Π , we simply obtain

$$\frac{d\rho}{dT} = - \left(\frac{\partial \Pi}{\partial \rho} \right)^{-1} \left[-A\ell\rho\gamma'(T)\nabla T + \frac{\partial \Pi}{\partial T} \right], \quad (31)$$

so that the Soret coefficient can be directly expressed as

$$S_T = -\frac{1}{\rho} \frac{d\rho}{dT} = K_T \left[-A\ell R\rho\gamma'(T) + \frac{\partial \Pi}{\partial T} \right] \quad (32)$$

where $K_T = \rho(\partial \Pi / \partial \rho)^{-1}$ is the osmotic compressibility of the suspension. Interactions therefore contribute to thermophoresis both by setting the overall amplitude, which is fixed by K_T , and by adding a collective term, related to the temperature derivative of Π . Proportionality with the osmotic compressibility, which is consistent with the data obtained for SDS in [18], has a simple physical meaning: repulsive interactions, lowering K_T , hinder the buildup of thermally induced concentration gradients, while the contrary happens for attractive interactions. Equation (32) shows that S_T depends only on *equilibrium* properties; since the Soret coefficient is the *ratio* of two transport coefficients, hydrodynamic factors are indeed expected to cancel out. Notice also that, without the driving force F_{th} , in the single-particle limit we would obtain $S_T = 1/T$, regardless of the specific nature of the investigated system. In addition, thermophoresis would be only a negligible $O(T^{-1})$ effect, while most of the data for S_T in macromolecular solutions or colloidal suspensions are at least one order of magnitude larger. This blatant contradiction with the experimental findings was pointed out by Soret himself while considering the explanation of thermal diffusion originally put forward by van't Hoff [36], who simply assumed uniformity of the osmotic pressure along the cell. Unfortunately, neglect of careful consideration of single-particle effects can still be found in recent papers on thermophoretic effects. Dhont for instance, in spite of an accurate analysis of collective effects on colloid thermophoresis, both from a statistical thermodynamics [37] and a microscopic hydrodynamics point of view [38], introduces a possible single-particle contribution only ‘in passing’, as an effect related to the temperature dependence of the particle chemical potential, without envisaging a physical driving force. Conversely, we have seen that single-particle effects constitute, in terms of magnitude, the core part of the Soret coefficient. I should point out, however, that Dhont’s expressions for D_T and D (equation (27) in [37]) yield the same collective contribution to S_T as in the present derivation. Similarly Chapman, in his original discussion of Brownian motion in thermal gradients [39] (where no effective external force on the particle was introduced) was not able to account for thermophilic behaviour. A recent critical reappraisal of the problem by Bringuier and Bourdon [40] does take into account interactions of the particle with its surroundings, and might give statistical mechanics bases to the present semi-phenomenological approach, but its results seem so far to be easily applicable only to (according to the authors’ definition) ‘toy models’.

7. Conclusions

Let me first summarize the key features of the approach I have followed.

- First of all, understanding thermally driven diffusion might be much simpler for colloidal suspensions or macromolecular solutions (in other words, what are commonly called ‘complex’ fluids) than for ‘simple’ liquid mixtures, the crucial reason being the wide separation of particle and solvent length scales, allowing the treatment of the latter as a continuum and using hydrodynamics.
- The main difference between an equilibrium flow problem, in the presence of a body external force, and phoretic motion is the need for introducing slip boundary conditions,

dictated by the thin inhomogeneous interfacial layer induced by the particle acting on the fluid as an external field. This feature directly links thermophoresis to the analysis of liquid structure near interfaces.

- In spite of the different energy transfer mechanism (which in gases is simply kinetic), many similarities exist between thermophoresis in liquids and gases: stresses are longitudinal, a characteristic length (λ for gases, ℓ for liquids) fixes the strength of the effect; the bulk particle properties enters only via the thermal conductivity.
- It is possible to ‘translate’ the thermal inhomogeneity into an effective external force acting on the particle, easily allowing the extension of the results to interacting particles. It is interesting that such a force is proportional to a simple interfacial thermodynamic property as the temperature derivative of γ . Therefore, if the *ansatz* we made holds true, thermophoresis might be considered as an interesting probe of particle/solvent interfacial properties.
- For the specific case of charged colloids at sufficiently high ionic strength ($\lambda_{\text{DH}} \ll R$), the model leads to analytical predictions in agreement with the experimental results for micellar systems.

Therefore, although they do not constitute yet a rigorous microscopic model of particle thermophoresis in liquids, the general ‘guidelines’ we have developed in the former sections represent a tool for guessing a possible microscopic interpretation of many of the experimental observations on specific systems. For instance, in the framework of the general model I have tried to outline, sign-reversal from $S_T < 0$ to $S_T > 0$ by raising T should imply, from (32), a maximum of the particle/solvent interfacial tension at intermediate temperature (unless more subtler effects, leading to a sign-reversal of ℓ , are present). Since, as I anticipated, this behaviour seems to be shared by a large number of aqueous systems, this feature should be related to general structural properties of water.

I stress again that all ideas that have been presented are restricted to situations where the thickness of the interfacial region is small compared to the particle size; in this case, the thermophoretic velocity should not depend on the particle size R , and the Soret coefficient should scale linearly with R . Explanation of the sign-reversal of S_T in charged systems for large values of the screening length is therefore precluded from the present model, and requires further consideration of curvature effects or, possibly, of interparticle interactions.

Finally, it would be interesting to investigate how this approach can be applied to polymer thermophoresis. Short-ranged coupling with the thermal field is indeed implicit both in the original argument leading to a molecular-weight independent D_T [41] (which seems to hold true also for short chains, in spite of foreseeable end effects [42]) and in the detailed analysis by Schimpf and Giddings [43]. One may for instance wonder whether for flexible *polyelectrolytes* at sufficiently low ionic strength, where strong inter-monomer charge coupling is expected, the latter feature is still retained.

Acknowledgments

I thank very much Benedetta Triulzi and Sara Iacopini, who performed the measurements presented in figure 1. I am also greatly indebted to Marzio Giglio, for invaluable experimental hints, and to Alberto Parola and Carlo Cercignani for useful suggestions and discussions. I finally wish to acknowledge the Italian Ministry for University and Research (MIUR) funding this research.

References

- [1] Ludwig C 1859 *S. B. Akad. Wiss. Wien* **20** 539
- Soret C 1879 *Arch. Sci. Phys. Nat.* **2** 48
- [2] Tyrrell J V 1961 *Diffusion and Heat Flow in Liquids* (London: Butterworths)
- [3] Zheng F 2002 *Adv. Colloid Interface Sci.* **97** 255
- [4] Giglio M and Vendramini A 1977 *Phys. Rev. Lett.* **38** 26
- [5] Zhang K J, Briggs M E, Gammon R W, Sengers J W and Douglas J F 1999 *J. Chem. Phys.* **111** 2270
- [6] Blums E, Odenbach S, Mezulis A and Maiorov M 1998 *Phys. Fluids* **10** 2155
- [7] Braun D and Libchaber A 2002 *Phys. Rev. Lett.* **89** 188103
- [8] Iacopini S and Piazza R 2003 *Europhys. Lett.* **59** 142
- [9] de Gans B-J, Kita R, Müller B and Wiegand S 2003 *J. Chem. Phys.* **118** 8073
- [10] Derjaguin B V and Sidorenkov G P 1941 *Dokl. Acad. Nauk SSSR* **32** 622
- [11] Derjaguin B V, Churaev N V and Muller V M 1987 *Surface Forces* (New York: Consultants Bureau) chapter 11
- [12] Ruckenstein E 1981 *J. Colloid Interface Sci.* **83** 77
- [13] Giglio M and Vendramini A 1974 *Appl. Phys. Lett.* **25** 555
- [14] Piazza R 2003 *Phil. Mag.* **83** 2067
- [15] Gordon J P, Leite R C C, Moore R S, Porto S P S and Whinnery J R 1965 *J. Appl. Phys.* **36** 3
- [16] Rusconi R, Isa L and Piazza R 2004 *J. Opt. Soc. Am. B* **21** 605
- [17] Corti M and Degiorgio M 1981 *J. Phys. Chem.* **85** 711
- [18] Piazza R and Guarino A 2002 *Phys. Rev. Lett.* **88** 208302
- [19] Piazza R 2000 *Curr. Opin. Colloid Interface Sci.* **5** 38
- [20] Piazza R, Iacopini S and Triulzi B 2004 *Phys. Chem. Chem. Phys.* **6** 1616
- [21] Triulzi B, Iacopini S and Piazza R 2004 in preparation
- [22] Brush S G 1976 *The Kind of Motion we Call Heat* vol 1 (Amsterdam: North-Holland) chapter 5
- [23] Kennard E H 1938 *Kinetic Theory of Gases* (New York: McGraw-Hill) chapter 8
- [24] Maxwell J C 1879 *Phil. Trans. R. Soc.* **170** 231
- [25] Tyndall J 1870 *Proc. R. Inst.* **6** 1
- [26] Epstein P S 1929 *Z. Phys.* **54** 537
- [27] Anderson J L 1989 *Annu. Rev. Fluid Mech.* **21** 61
- [28] Dariel M S and Kedem O 1975 *J. Phys. Chem.* **79** 336
- [29] Haase R and de Greiff H J 1965 *Z. Phys. Chem. Frankfurt* **44** 301
- [30] Davis H T and Scriven L E 1982 *Adv. Chem. Phys.* **49** 357
- [31] Vervey E J W and Overbeek J T G 1948 *Theory of the Stability of Lyophobic Colloids* (New York: Elsevier)
- [32] Alexander S *et al* 1984 *J. Chem. Phys.* **80** 5776
- [33] Bucci S, Fagotti C, Degiorgio V and Piazza R 1991 *Langmuir* **7** 824
- [34] Morozov K I 1999 *JETP* **88** 944
- [35] Landau L D and Lifshitz E 1987 *Fluid Mechanics* 2nd edn (New York: Pergamon)
- [36] van't Hoff J H Z 1887 *Z. Phys. Chem.* **1** 481
- [37] Dhont J K G 2004 *J. Chem. Phys.* **120** 1632
- [38] Dhont J K G 2004 *J. Chem. Phys.* **120** 1642
- [39] Chapman S 1928 *Proc. R. Soc. A* **119** 34
- [40] Bringuier E and Bourdon A 2003 *Phys. Rev. E* **67** 011404
- [41] Brochard F and De Gennes P-G 1981 *C. R. Acad. Sci. II* **293** 1025
- [42] Wiegand S 2004 *J. Phys.: Condens. Matter* **16** R357
- [43] Schimpf M E and Giddings J C 1987 *Macromolecules* **20** 1561